

Analysis of Fatigue Life and Crack Growth in Austenitic Stainless Steel AISI 304L

Lotfi CHELBI, Fatma HENTATI*, Amna ZNAIDI

Applied Mechanics and Engineering Laboratory (LR-MAI), National Engineering School of Tunis ENIT, Tunis, 1002, Tunisia

Received 29 Jul 2023

Accepted 29 Sep 2023

Abstract

This paper focuses on life prediction models considering the variability of loads. It describes the fatigue strength and crack growth behavior of AISI 304L austenitic stainless steel at room temperature. The deformation behavior of the austenitic stainless steel was investigated via tensile and fatigue tests. Crack tests were performed on CT50 specimens for constant ΔP and ΔK under different cyclic loads before the specimen was severely cracked by a monotonically increasing load. The impact of loading sequence and the evolution of the dissipated energy ΔJ were investigated using constant charge ΔP and stress intensity ΔK . The dissipated energy per cycle is used to predict fatigue crack growth. Experimental results proved that the various parameters considered in terms of cyclic loading and the results obtained under monotonic loading up to unstable failure show that cracking at constant ΔP is significantly more damaging than at constant ΔK . Therefore, cyclic loading with a constant pressure drop will result in faster crack growth or shorter fatigue life than loading with a constant stress intensity factor ΔK .

© 2023 Jordan Journal of Mechanical and Industrial Engineering. All rights reserved

Keywords: Austenitic Stainless Steel AISI 304L / Fatigue crack growth/Stress intensity factor range ΔK / Loading charge ΔP /Dissipated Energy ΔJ / Monotonic, cyclic loadings.

Nomenclature

σ_u	Ultimate tensile strength	E	Young's modulus
σ_{y0}	Yield strength	B	Thickness of the CT specimen.
a	Crack length	$\frac{a}{w}$	Crack growth fatigue rate.
W	Width of the CT specimen	K	Stress intensity factor.
ΔK	Stress intensity factor range.	ΔP	Applied load range.
P	Applied load	ΔJ	Dissipated energy.
R	Load ratio	ΔJ_p	Dissipated energy at constant ΔP .
ΔJ_K	Dissipated energy at constant ΔK	COD	Crack Opening displacement

1. Introduction

Austenitic stainless steels are often used as reactor materials for chemical plants due to their high corrosion resistance and workability as well as their good weldability. These materials are used extensively in the nuclear industry due to their good mechanical properties such as ductility and work hardening, as well as their corrosion resistance [1-5]. The effect of a material's deformation or loading history on subsequent cyclic

loading depends on the degree of cyclic strain hardening, which in turn depends on how easily the dislocations can cross over [6-11]. Some researchers such as Cruces and others studied the influence of deformation history on the fatigue behavior of 316 and 304 austenitic stainless steels [12]. Kant C and al [13] investigated the life prediction models considering the variability of fluctuating loads. In their study, the modes were based on the concept of crack propagation, load interaction, number of cycles, stress and variable amplitude loading with crack closure. In another work of Kant C and al [14], used the AISI30L for various overload ratio and crack length to explore the effect on fatigue crack propagation. The impact of scattered overload under constant amplitude loading is simulated by a modified virtual crack annealing (MVCA) model based on crack closure phenomena. Moreover, Kant C and al [15] conducted a comparative study of analytical fatigue crack propagation models under the effect of interspersed overload in constant amplitude loading. The influence of interspersed overload induced retardation was pretended by crack closure model MVCA (Modified virtual crack annealing), plasticity zone interaction models (Wheeler model). These scholars estimated the life of the austenitic stainless steel AISI304L via linear elastic fracture mechanics-based Paris model. In parallel, Colin and Co [16] studied the effects of deformation history on 304L stainless steel due to pre-hardening, as well as the effects of mean stress and mean strain and the effects of load sequence on fatigue life. Lehéricy Y [17] has also demonstrated the influence of pre-hardening and loading sequence on the deformation and fatigue behavior of materials with a significant effect of deformation history,

* Corresponding author e-mail: fatma.hentati1@gmail.com.

where the amplitude of preload and overload cycles are the key parameters for material behavior. Nalepka and others [18] used cylindrical tensile and torsional specimens in accordance with a loading program to study the development of microstructure caused by a complex stress condition. They studied the evolution of the microstructure and its coupling with fracture under complex loading conditions at the temperature of liquid helium. Brittle fracture of structural components is usually analyzed using the stress intensity factor K , which quantifies the stress singularity at the crack tip. Moreover, fatigue crack growth analysis usually assumes that the crack driving force is the range of stress intensity factor ΔK [19]. This parameter is often used because there are analytical solutions for the standard samples, so the experimental work does not necessarily have to be done by numerical modeling. Also, it quantifies the effect of crack size and load level on stress singularity, facilitating the comparison of results on fatigue crack growth [20]. In another paper, the plastic CTOD range δ_p , which quantifies the plastic deformation of the crack tip, is used to study fatigue crack propagation instead of the classical elastic ΔK parameter [21]. For 304L stainless steel, $da/dN-\delta_p$ model was defined and determined experimentally using a standard specimen CT, while δ_p was predicted numerically using the finite element method [22]. Kumar et al [23] also showed that fatigue crack propagation in L-PBF 304L steel does not depend on structural orientation. They showed a significant effect of stress-induced martensitic transformation in the plastic zone of the crack tip on the crack opening displacement (COD) and hence on the crack propagation rate. Similarly, Vincent et al [24] studied fatigue experiments with high cycles at constant amplitude to characterize the mechanical behavior of the material as well as its fatigue resistance under the most common loading conditions. Other researchers like Cojocaru and Karlsson [25] have qualitatively demonstrated that dissipated energy can predict crack growth retardation after an overload. In parallel, Klingbeil [26] proposed a theory for fatigue crack growth based on the rate of plastic energy dissipation at the crack tip. The dissipated energy was calculated from a 2D elastic-plastic finite element analysis of a steady-state crack and used to predict the fatigue crack growth rates of various ductile metals under constant amplitude loading. Another approach involved finite element and constitutive models. For instance, Al Mukhtar et al [27] developed a new analytical approach for the weld to crack in cruciform welded joints to analyze the cracked body and describes the singularity at a head of the crack tip. Gharaibeh M.A [28] used symmetry-based finite element models for board-level electronic assemblies subjected to various types of loading. ANSYS commercial software was used for the quarter-symmetric model and the full models to perform all types of analysis. Also, Arumugan A et [29] investigated the analyses of spot weld failures experimentally and numerically using finite element analysis. The results found that welded joints have better fatigue life compared to spot welded joints.

In the present study, the influence of loading history of AISI 304L austenitic stainless steel on crack growth is investigated. The selected steel is used for various applications in different industries and is therefore an ideal candidate to study the effects of cyclic and monotonic loading and to predict fatigue life. The evolution of dissipated energy under cyclic and monotonic loading at constant stress intensity factor ΔK and charge ΔP is studied to explore the growth of crack propagation in order to estimate the fatigue life of the austenitic steel. The experimental data obtained in this work is a useful resource for the development and verification of numerical codes.

2. Experimental set up

2.1. Material

Due to its good corrosion resistance and high plasticity, Austenitic Stainless Steel AISI 304L, commonly adopted in primary circuits of nuclear reactors, was used in this study. All the specimens employed for the various tests were hardened at 1070°C. The chemical compositions, in weight percent, of steel are given in Table 1.

Table 1. Chemical composition of type AISI 304L stainless steel (in wt. %).

C	Mn	P	S	Si	Cr	Ni	N
0.048	1.420	0.030	0.009	0.550	18.100	8.570	0.038

2.2. Mechanical characterization tests

The tensile test presents the most important fundamental test which can be performed on material. Tensile tests are simple, relatively inexpensive, and fully standardized. The tests were carried out on work pieces at room temperature and strain rate of $4 \cdot 10^{-4}$ m/min. The load-deflection curves were obtained based on the true stress – strain curves. To determine the tensile properties of the materials, specimens were machined to the dimensions given in Figure 1 according to ASTM F138 for steel. The tensile tests were repeated three times, and then the average of load-deflection was calculated.

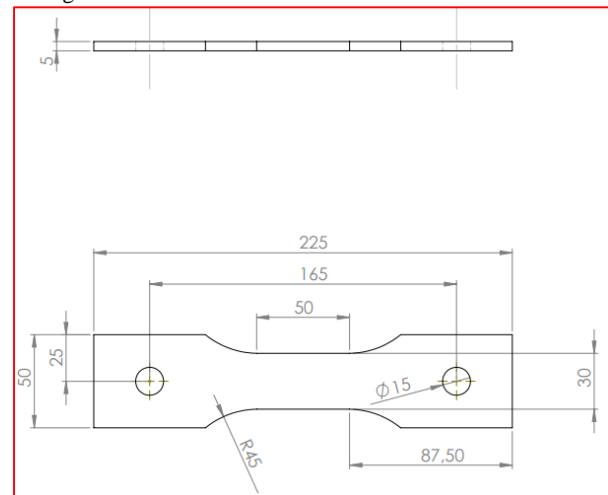


Figure 1. Geometry and dimensions (in mm) of the tensile specimen.

The basic mechanical properties are listed in Table 2. The experimental tests are carried out with a servo-hydraulic machine MTS with a dynamic capacity of ± 25 tones, provided with a micro-console for control load, displacement and deformation. The MTS machine is equipped with an acquisition chain type HP, which receives a predefined software for tensile, fatigue or room temperature-high temperature fatigue tests. At room temperature, cracking is checked using a video camera system that detects the crack and displays it immediately on a screen.

Table 2. Mechanical properties of type AISI 304L stainless steel.

σ_{y0}	σ_u	E	Hardness HRB	Poisson Coefficient ν
MPa	MPa	MPa	–	–
292	633	$189 \cdot 10^3$	82	0.3

The fatigue crack growth rate was determined on standard tensile specimens CT50. The geometry of the crack specimens used is according to the ASTM-E399. The dimensions and tolerances are illustrated in Figure 2, and herringbone notches were incorporated in the casting crack of the different specimens to optimize the time of pre-cracking. These specimens were machined so that the crack direction was in the rolling direction. These tests are characterized by stable cracks up to a compliance (a/w) and constant loading charge ΔP and stress intensity range ΔK before the unstable fracture occurs.

2.3. Experimental protocol

Fatigue tests were performed in an Instron servo-hydraulic testing machine under load control with a sinusoidal wave form with a frequency of 20 Hz and the R-ratio for the constant amplitude loading was kept to be 0.1. The crack length was measured by the change in the compliance (a/w) curve measured with a gauge COD according to ASTM recommendations.

The various crack tests were performed under cyclic and monotonic stresses at constant ΔP and ΔK to better identify the effects of the loading history on the AISI 304L material.

The load ratio is calculated as follow:

$$R = \frac{K_{\min}}{K_{\max}} \tag{1}$$

$$\Delta K = K_{\max} - K_{\min} \tag{2}$$

$$K_{\max} = \frac{\Delta K}{R} \tag{3}$$

For the three ΔK values chosen, the variation of the maximum stress σ_G as a function of crack length during propagation were recorded. The maximum stress σ_G derived from relation (4) is a function of the compliance and the load P applied during crack formation. This load decreases with time to reach a constant level ΔK .

The maximum stress is defined as below:

$$\sigma_G = \frac{K_{\max}}{f\left(\frac{a}{w}\right)\sqrt{w}(1-R)} \tag{4}$$

The stress intensity factor K was determined using a closed solution as follows:

$$K = \frac{P}{B\sqrt{w}} f\left(\frac{a}{w}\right) \tag{5}$$

Where:

K: the stress intensity factor.

P: the applied load.

w: the width of CT specimen.

a: crack length.

B: thickness of CT specimen.

The Paris Law is a well-known empirical equation used to describe fatigue crack growth behavior. It is often written as:

$$\frac{da}{dN} = C.(\Delta K)^n \tag{6}$$

Where:

da: the change in crack length per cycle.

dN: the number of cycles.

C and n are material dependent constants.

ΔK : the stress intensity factor range, related to ΔP and the crack geometry.

An opening sensor (COD), a load cell of a servo machine (MTS), and a plotter to record force-displacement curves (P, δ) were used to measure ΔJ for cyclic and monotonic loadings. Two types of COD sensors were used, one with a maximum aperture of 3 mm for stable fracture and the other with a maximum aperture of 9 mm for unstable fracture. The sensor is placed on both sides of the crack lips and the (P, δ) curves are recorded for a given load.

The tests involve stable cracking at ΔP or ΔK up to a given value of a_0/w before tearing or unstable material failure. The crack propagation is monitored using a COD camera.

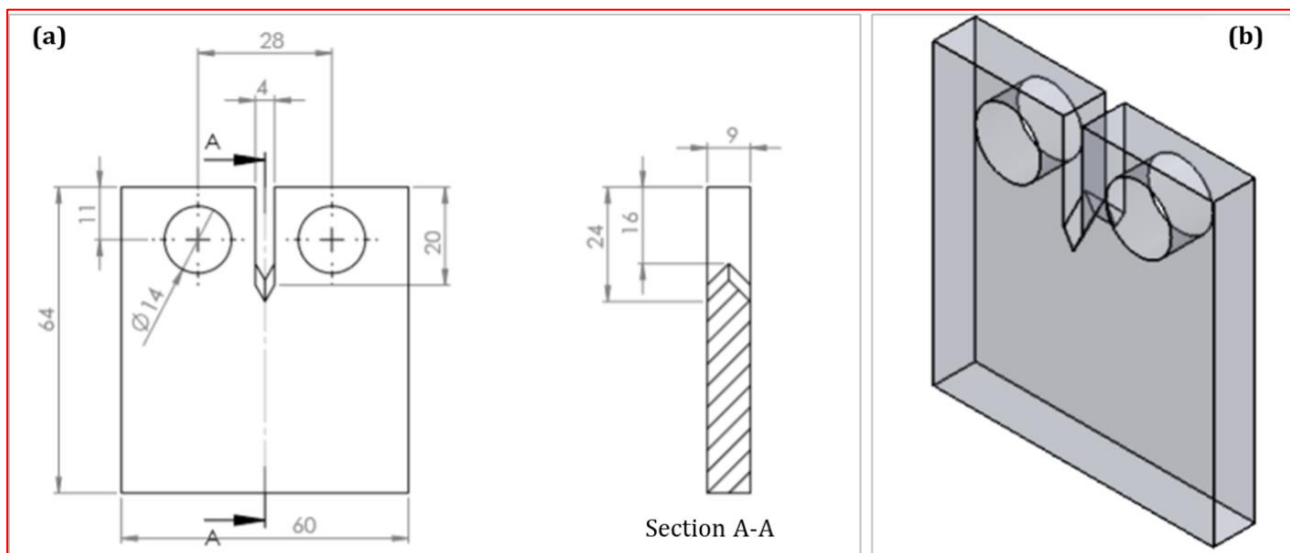


Figure 2. Geometry and dimensions (in mm) of the standardized CT-50 specimen, (b) The isometric view of the specimen.

For cyclic loading, the value of ΔJ depends on the area that covers the part beyond the crack closure point relative to the load-displacement diagram (P, δ) as shown in Figure 3.

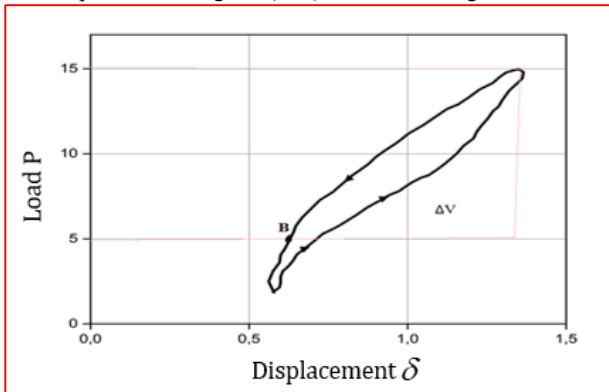


Figure 3. Load P as a function of displacement δ .

Hence, J is calculated as follows:

$$\Delta J = \frac{\Delta K_e}{E} + \frac{\Delta V}{2aB} \tag{7}$$

Where:

ΔK_e : amplitude of the effective stress intensity factor,

corresponding to ΔP_e for the mode I for failure.

ΔV : surface of the hysteresis loop measured from the closing point of the load-displacement diagram.

E: Young's Modulus.

The evolution of the work dissipated during stable or unstable failure, expressed by the integral J. The measurements are based on several load-displacement curves.

Under monotonic loading, cracking to unstable failure, a 9 mm COD opening sensor is used to record the (P, δ) curves. An image processing system is used to follow the evolution of the highly deformed zone at the end of the crack (plastic zone).

For each treatment of the load-displacement curves, the existing area supported by the curve (P, δ) shown in Figure 4, is integrated and the final values of ΔJ are calculated using equations (7) and (8).

$$J = \left(\frac{1+\alpha}{1+\alpha^2} \right) \frac{2A}{Bb} \tag{8}$$

With:

A: surface under the curve load-displacement (P, δ).

b: length of ligament left after cyclic loading.

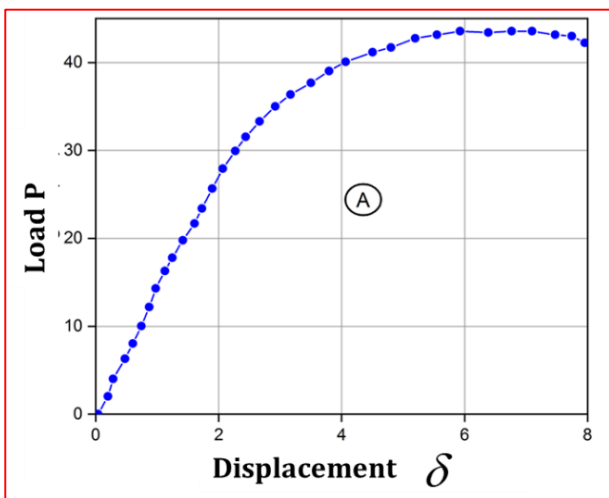


Figure 4. Load-displacement diagram recorded under monotonic loading after pre-cracking.

3. Results and discussions

3.1. Analysis of the dissipated energy under cyclic loading

The dissipated energy ΔJ measurements are performed for three stress intensity factor range ΔK values that define the crack range (da/dN) for the stainless-steel material used. The ΔK values investigated are: 30, 60 and 80 $MPa\sqrt{m}$. The impact of three different stress intensity factor ΔK values on the evolution of dissipated energy as a function of crack length is depicted in Figure 5, and can be described as follows: To begin with ΔK_1 , the dissipated energy curve typically exhibits a gradual and relatively flat slope as a function of crack length. ΔJ increases slowly with crack length, indicating that the material does not undergo significant energy loss as the crack extends. This proves that the material is relatively tough and can withstand the applied load without rapid fracture. In this case, the applied load is not sufficient to cause rapid crack propagation [24, 30, 31].

With a moderate stress intensity factor relative to ΔK_2 , the applied load is more significant, and the material is closer to the point of fracture initiation. The dissipated energy curve will exhibit a steeper slope as a function of crack length compared to the ΔK_1 case [30-32]. As the crack propagates, the dissipated energy increases at a faster rate, indicating that more energy is being lost as the crack propagates. This indicates that the material is undergoing significant energy dissipation and is approaching a critical condition for fracture.

At ΔK_3 , the applied load is close to or exceeds the critical stress intensity factor (K_c) for the material, leading to rapid crack propagation. The dissipated energy curve will exhibit a very steep increase as a function of crack length, potentially with a sharp peak followed by a rapid drop. As the crack extends, a significant amount of energy is rapidly dissipated, signifying brittle fracture. High ΔK values indicate that the material's toughness may not be sufficient to resist the applied load, and fracture occurs rapidly [33].

The analysis of fatigue crack growth usually assumes that the crack driving force is the range of stress intensity factor, ΔK . This parameter quantifies the effect of crack size and load level on stress singularity [34-37].

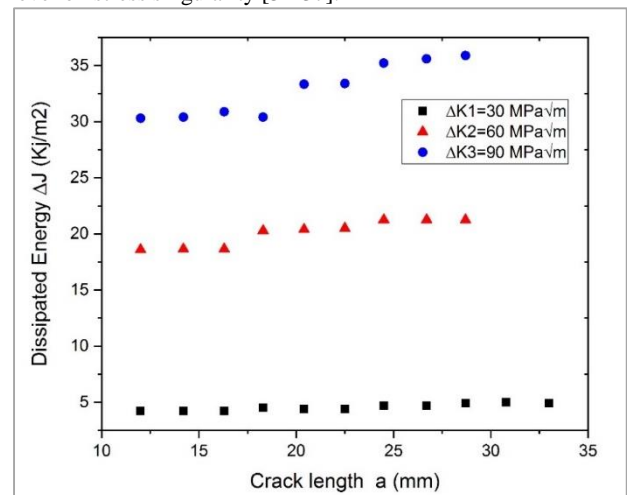


Figure 5. Dissipated energy ΔJ as a function of crack length under constant intensity factor ΔK .

The variation of dissipated energy as a function of crack length under cyclic loading depends significantly on the applied loading conditions. The ΔP values studied are: 9300, 13320 and 27720 N. The impact of three different loading ΔP values (low, moderate, and high) on the dissipated energy as a

function of crack length for cyclic loading cycles is depicted in Figure 6.

When the cyclic loading is relatively low, i.e. ΔP_1 , it means that the applied stress levels are not very high, and the loading may not be sufficient to promote rapid crack propagation. Under low loading conditions, ΔJ accumulates slowly with crack length. Hence, the material exhibits better fatigue resistance, and the dissipated energy remains relatively low even after many loading cycles [30, 35-38].

At ΔP_2 , the applied stress levels are higher than in the low loading case (ΔP_1), and the material is more susceptible to crack growth. The dissipated energy curve shows a steeper increase as a function of crack length compared to the low loading scenario under cyclic loading. As the crack propagates during each loading cycle, the dissipated energy increases at a faster rate, indicating that more energy is being lost as the crack propagates. Therefore, the material may still exhibit reasonable fatigue life, but the dissipated energy becomes more pronounced with each load cycle, increasing the risk of fatigue failure [30, 37-39].

At the third load ΔP_3 , the applied stresses are close to or above the fatigue limit of the material, resulting in rapid crack propagation. As the crack expands during each loading cycle, a significant amount of energy is dissipated rapidly, resulting in rapid crack growth and increased risk of premature fatigue failure. High loading conditions significantly reduce the fatigue life of the material, and the dissipated energy accumulates rapidly with each loading cycle, making the component susceptible to early failure [30, 40, 41].

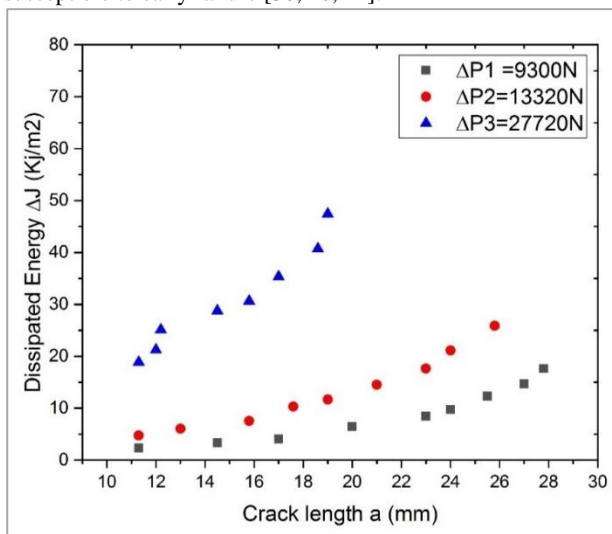


Figure 6. Dissipated energy ΔJ as a function of crack length under constant cyclic loading ΔP .

3.2. Analysis of the dissipated energy under monotonic load

After cracking at constant ΔP and ΔK for a given crack length, all specimens exhibiting greater damage are subjected to increasing monotonic loading until they suddenly fracture.

Stable cracking is performed for four crack lengths a_0 before unstable fracture of the material under test is induced. These lengths correspond respectively to the values: 12.5, 20, 25 and 30 millimeters for each case of the measurement. The ratios (a/w) are respectively: 0.25, 0.40, 0.50 and 0.60 to define the compliance function $f(a/w)$ of the specimen CT.

According to the results in Figure 7, the effect of monotonic loading on the energy dissipated during unstable fracture are demonstrated and described.

The stress intensity factor ΔK_1 is relatively low, the applied load is not sufficient to produce rapid crack propagation. Under monotonic loading conditions, the dissipated energy curve as a function of crack length typically shows a gradual and relatively flat slope. ΔJ accumulates slowly with crack length, indicating that the material is not undergoing significant energy loss as the crack extends. Therefore, the material is less susceptible to fracture, and the dissipated energy remains relatively low even as the crack expands [30, 34, 35].

With a stress intensity factor ΔK_2 , the dissipated energy shows a steeper increase as a function of crack length compared to the low ΔK_1 case under monotonic loading. As the crack propagates, the dissipated energy increases at a faster rate, indicating that more energy is being lost as the crack propagates. For moderate ΔK values, the material is more susceptible to crack growth, and energy dissipation becomes more pronounced as the crack extends.

When the stress intensity factor ΔK_3 is high, the applied load is close to or exceeds the critical stress intensity factor (K_c) for the material, leading to rapid crack propagation. The dissipated energy curve under high ΔK_3 values depicts a very steep increase as a function of crack length, potentially with a sharp peak followed by a rapid drop. As the crack extends, a significant amount of energy is rapidly dissipated, signifying brittle fracture. High ΔK values indicate that the material's toughness may not be sufficient to resist the applied load, and fracture is imminent. To conclude, the stress intensity factor ΔK has a direct influence on the rate of energy dissipation in the propagation of a crack under monotonic loading conditions [30, 41, 42].

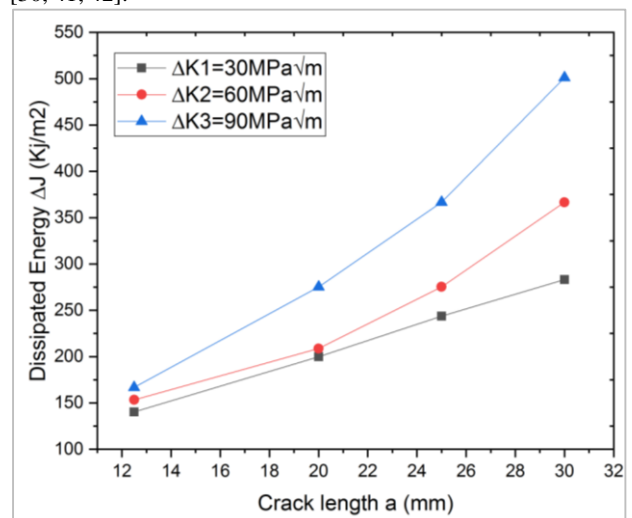


Figure 7. Variation of dissipated energy ΔJ as a function of crack length at constant ΔK .

At the first loading ΔP_1 , the dissipated energy curve as a function of crack length will typically exhibit a gradual and relatively flat slope. The material experiences relatively low stress levels during the monotonic loading cycle. The dissipated energy accumulates slowly with crack length, indicating that the material is not undergoing significant energy loss as the crack extends. For ΔP_1 , the material is less prone to catastrophic fracture, and the dissipated energy remains relatively low even as the crack extends [30, 43].

Moderate loading ΔP_2 increase the amplitude of cyclic loading, resulting in higher stress values during the monotonic loading cycle. The dissipated energy curve shows a steeper increase as a function of crack length compared to the case of low loading ΔP_1 during monotonic loading. As the crack length increases, the dissipated energy increases more rapidly, indicating that more energy is lost as the crack propagates. At

moderate loading, the material is more susceptible to crack growth, and energy dissipation becomes more pronounced as the crack length increases.

At high loading ΔP_3 , the amplitude of the cyclic loading is significantly high, resulting in very high stress levels during the monotonic loading cycle. The dissipated energy curve under high loading charge will exhibit a very steep increase as a function of crack length. As the crack extends, a significant amount of energy is rapidly dissipated, signifying brittle fracture. High loading charge conditions reduce the material's ability to resist catastrophic fracture, and the dissipated energy accumulates rapidly as the crack extends [30, 40-44].

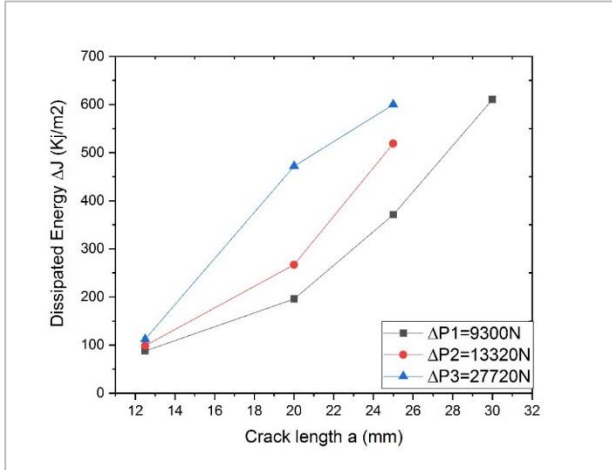


Figure 8. Variation of dissipated energy ΔJ as a function of crack length at constant ΔP .

3.3. Evolution of dissipated energy

The evolution of the dissipated work or the course of the stable or unstable fracture is expressed by the integral J. The experimental results of the cracking tests at ΔK and ΔP constant show that the evaluation of the dissipated energy ΔJ is active and fast when the loading is carried out at constant ΔP .

The evolution of ΔJ can be directly related to the crack reinforced and to the extent of the plastic region that develops at the crack tip. These measurements confirm the results concerning the evolution of the curve $(da/dN-\Delta K)$ obtained on the same material [30, 44, 45].

It can be admitted that under cyclic loading the dissipated energy ΔJ follows developments of the type:

$$\Delta J_K = a_{1c} a^{n_{1e}} \tag{9}$$

$$\Delta J_P = a_{2c} a^{n_{2e}} \tag{10}$$

Figures 9 and 10 reported here show an exponent n_{1c} that is significantly lower than n_{2c} , suggesting an essentially constant crack growth rate at constant ΔK . Under monotonic loading after crack growth at constant ΔK and ΔP , the dissipated energy ΔJ reached critical values that were 100 to 200 times higher than the values obtained under cyclic loading. This has led us to limit the study of the effects of history to the load amplitudes ΔP_1 , ΔP_2 , and ΔP_3 .

For cyclic loading, the dissipated energy ΔJ will exhibit variations within each loading cycle, but the average ΔJ value can remain relatively constant as long as the ΔK value is maintained. However, for monotonic loading, ΔJ increases steadily with increasing crack length due to the constant range of the stress intensity factor [30, 32, 46-48].

The main difference between the evolution of dissipated energy ΔJ under cyclic and monotonic loading is the cyclic

nature of loading and unloading under cyclic loading, which can lead to hysteresis-like behavior and fluctuations of ΔJ . In contrast, monotonic loading results in a more straight-line and steady increase in ΔJ with crack length. When ΔK is held constant, the behavior of ΔJ is affected by the loading mode (monotonic or cyclic), but is relatively stable as long as ΔK remains constant [47, 48].

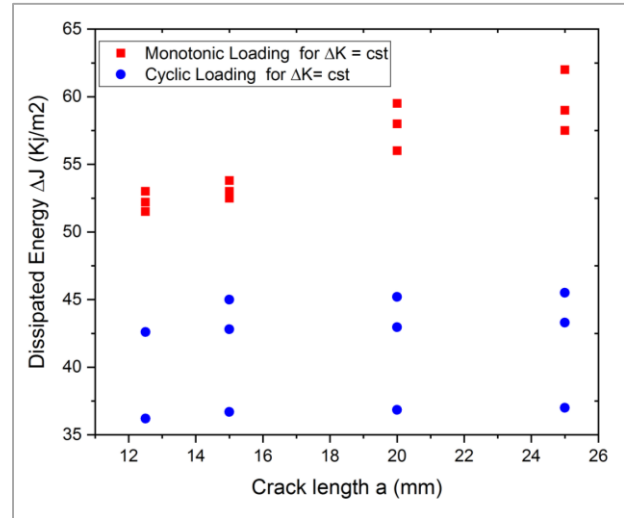


Figure 9. Evolution of dissipated energies ΔJ as a function of crack length until the crack at ΔK constant.

In the case of large deformations, the assumptions of bounded plasticity are no longer checked, and the singularity of the constraints is strongly modified. If this singularity is $1/\sqrt{(r)}$ for linear elasticity, it is weaker for plasticity and has the value $(n/(n+1))n$, i.e., the value of strain hardening and the value 0.16 for the austenitic stainless-steel material AISI 304L studied. This plastic singularity is well described by the J integral in a number of cases. The energetic meaning of J is based on the schematization of the elastoplastic real behavior with work hardening by the nonlinear elastic behavior. Consequently, the real meaning of J as a rate of energy release is limited.

Asymptotic solutions that give the distribution of stresses and strains using J are very useful when combined with a more realistic solution at the crack tip to describe the blunting of the crack, which itself is a function of the applied loading history. The approximate methods for evaluating J based on limit load considerations have allowed us to easily calculate this parameter [40-44].

All these reasons contribute to consolidate recent developments in fracture mechanics in nonlinear behavior by relying on the parameters J, even in imperfect and insufficiently justified applications. The determination of a critical J (J_{1c}) is sufficient to determine the initial point of propagation, which, however, continues only when a sudden release of energy occurs [42-45].

According to our experimental results, focusing on the AISI304L steel considering ASTM recommendations ($a/w=0.5$), the value of J_{1c} ranges from 243.7 to 366.6 (J/m^2) after scribing at constant ΔK and from 371 to 519 (J/m^2) after scoring at constant ΔP .

It is clearly seen in Figure 10, that for monotonic loading, where the load is applied continuously until failure, keeping ΔP constant (plastic region) means that the dissipated energy ΔJ increases as the crack progresses. In this case, more plastic deformation occurs and therefore more energy is dissipated. For monotonic loading, the dissipated energy ΔJ increases steadily with crack length, while ΔP remains constant. Under cyclic loading, energy is dissipated due to crack propagation and plastic deformation, but some of this energy can be

recovered during unloading. The ΔJ vs. crack length curve under cyclic loading with constant ΔP is likely to exhibit fluctuations within each cycle and may exhibit cyclic or hysteresis-like behavior depending on the loading conditions [40-42, 46-50].

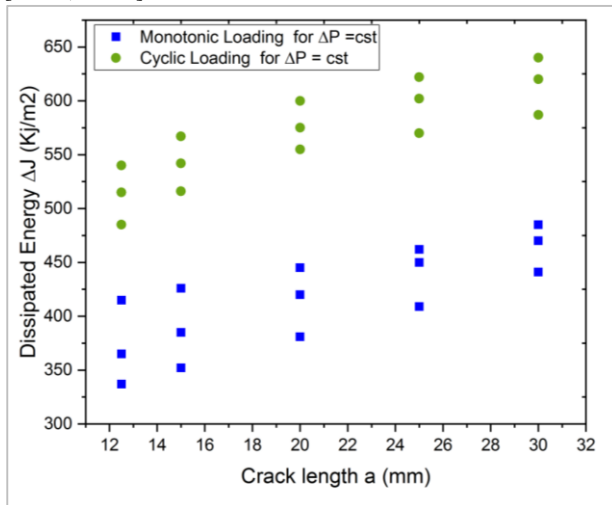


Figure 10. Evolution of the dissipated energies ΔJ as a function of crack length until the crack at ΔP constant.

4. Conclusions

Fatigue crack growth analysis was carried out on different variable loading cases using three CT specimens per test case. A video camera was used to follow and monitor the crack propagation of the material studied AISI304L during the fatigue testing. The evolution of the dissipated energy under cyclic and monotonic loadings for constant stress intensity factor range ΔK and loading charge ΔP are investigated to explore the crack propagation's growth. The dissipated energy can account for both crack tip plasticity and plastic-induced crack closure, and is therefore an excellent parameter for predicting fatigue crack growth after fatigue test overload. In addition, the approach provides the opportunity to learn more about how the fatigue crack growth of a material is affected by the underlying mechanical properties. Experimental results proved that the various parameters considered in terms of cyclic loading and the results obtained under monotonic loading up to unstable failure show that cracking at constant ΔP is significantly more damaging than at constant ΔK . Therefore, cyclic loading with a constant pressure drop will result in faster crack growth or shorter fatigue life than loading with a constant stress intensity factor ΔK . Finally, we recommend that future works involve the exploitation of the experimental results to create a valuable resource for the development and verification of numerical codes.

References

- [1] P. Jovicevic-Klug, M. Jovicevic-Klug, M. Rohwerder, M. Godec, B. Podgornik, "Complex Interdependency of Microstructure, Mechanical Properties, Fatigue Resistance, and Residual Stress of Austenitic Stainless Steels AISI 304L". *Materials*, Vol. 16, No. 7, 2023, 2638.
- [2] M. F. Mc Guire, *Stainless steels for design engineers*. Asm International; 2008.
- [3] N. Alshabat, S. Al-qawabah, "Effect of 4% wt. Cu Addition on the Mechanical Characteristics and Fatigue Life of Commercially Pure Aluminum". *Jordan Journal of Mechanical and Industrial Engineering*, Vol 9, No. 4, 2015.
- [4] N.R. Baddoo, "Stainless steel in construction: A review of research, applications, challenges and opportunities". *Journal of Constructional Steel Research*, Vol 64, No. 11, 2008, 1199-1206.
- [5] B. S. Reddy, J. S. Kumar, K. V. K. Reddy, "Prediction of surface roughness in turning using adaptive neuro-fuzzy inference system". *Jordan Journal of Mechanical and Industrial Engineering*, Vol 3, No. 4, 2009, 252-259.
- [6] Z. X. Yang, Y.F. Mai, "Steering Rod Fatigue Test Bench Cam Loading Analysis". *Jordan Journal of Mechanical and Industrial Engineering*, Vol 6, No. 2, 2012.
- [7] S. Agarwal, S. Chakraborty, K. Prasad, S. Chakraborty, "A rough multi-attributive border approximation area comparison approach for arc welding robot selection". *Jordan Journal of Mechanical and Industrial Engineering*, Vol 15, No. 2, 2021.
- [8] H. Eskandari, "Three-Dimensional Investigations of Stress Intensity Factors in a Rotating Thick-Walled FGM Cylinder". *Jordan Journal of Mechanical and Industrial Engineering*, Vol 10, No. 2, 2016.
- [9] K. Al bkoor Alrawashdeh, N.S. Gharaibeh, A.A. Alshorman, M.H. Okour, "Magnus Wind Turbine Effect Vertical Axis Using Rotating Cylinder Blades". *Jordan Journal of Mechanical and Industrial Engineering*, Vol 15, No. 2, 2021, 233-241.
- [10] M. H. Obaidat, O. T. Al Meanazel, M. A. Gharaibeh, H. A. Almomani, "Pad Cratering: Reliability of Assembly Level and Joint Level". *Jordan Journal of Mechanical and Industrial Engineering*, Vol 10, No. 4, 2016.
- [11] E. A. Teshnizi, M. Jahangiri, A. A. Shamsabadi, L. M. Pomares, A. Mostafaeipour, M. E. H. Assad, "Comprehensive Energy-Econo-Enviro (3E) Analysis of Grid-Connected Household Scale Wind Turbines in Qatar". *Jordan Journal of Mechanical and Industrial Engineering*, Vol 15, No. 2, 2021.
- [12] AS. Cruces, P. Lopez-Crespo, S. Bressan, T. Itoh, "On the behaviour of 316 and 304 stainless steel under multiaxial fatigue loading: application of the critical plane approach", *Metals*, Vol 9, No. 9, 2019, 978.
- [13] C. Kant, G.A. Harmain, "A model based study of fatigue life prediction for multifarious loadings". *Key Engineering Materials*, Vol. 882, 2021, 296-327.
- [14] C. Kant, G.A. Harmain, "Analysis of single overload effect on fatigue crack propagation using modified virtual crack annealing model." *Recent Developments in Mechanics and Design: Select Proceedings of INCOME 2021*. Singapore: Springer Nature Singapore, 2022, p. 1-8.
- [15] C. Kant, G.A. Harmain, "Fatigue life prediction under interspersed overload in constant amplitude loading spectrum via crack closure and plastic zone interaction models—a Comparative Study". *Fracture, Fatigue and Wear*. Singapore: Springer Singapore, 2021. p. 253-260.
- [16] J. Colin, A. Fatemi, "Variable amplitude cyclic deformation and fatigue behaviour of stainless steel 304L including step, periodic, and random loadings". *Fatigue & Fracture of Engineering Materials & Structures*, Vol. 33, No. 4, 2010, 205-220.
- [17] Y. Lehericy, J. Mendez, "Effect of low cycle fatigue damage on the residual fatigue strength of 304L austenitic stainless steel". 9th International fatigue congress, Atlanta, GA, 2006.
- [18] K. Nalepka, B. Skoczeń, R. Schmidt, M. Ciepiewska, "Microstructure evolution in the context of fracture in austenitic steels under complex loads at cryogenic temperatures". *Materials Characterization*, Vol. 197, 2023, 112654.
- [19] J.R. Rice, "Mechanics of crack tip deformation and extension by fatigue". *Fatigue crack propagation*. Philadelphia: ASTM STP, Vol. 415, 1967, 256-71.
- [20] P.C. Paris, J. Erdogan, "Critical analysis of crack growth propagation laws". *Journal Basic Engineering*, Vol.185, No. 5, 1963, 528-533.
- [21] F.V. Antunes, R. Branco, P. Prates, C. Gardin, "Fatigue crack growth versus plastic CTOD in the 304L stainless steel". *Engineering Fracture Mechanics*, Vol. 214, 2019, 487-503.
- [22] T. Zhao, J. Zhang, Y. A. Jiang, "Study of fatigue crack growth of 7075-T651 aluminum alloy". *International Journal of Fatigue*, Vol. 30, No. 7, 2008, 1169-1180.

- [23] P. Kumar, R. Jayaraj, Z. Zhu, R.L. Narayan, "Role of metastable austenite in the fatigue resistance of 304L stainless steel produced by laser-based powder bed fusion". *Materials Science and Engineering: A*, Vol. 837, 2022, 142744.
- [24] L. Vincent, J.C. Le Roux, S. Taheri, "On the high cycle fatigue behavior of a type 304L stainless steel at room temperature". *International Journal of Fatigue*, Vol. 38, 2012, 84-91.
- [25] A.M. Karlsson, D. Cojocaru, "Assessing plastically dissipated energy as a condition for fatigue crack growth". *International Journal of Fatigue*, Vol. 31, No. 7, 2009, 1154-1162.
- [26] N.W. Klingbeil, "A total dissipated energy theory of fatigue crack growth in ductile solids". *International Journal of Fatigue*, Vol. 25, No. 2, 2003, 117-128.
- [27] A. M. Al-Mukhtar, S. Henkel, H. Biermann, P. Hübner, "A finite element calculation of stress intensity factors of cruciform and butt-welded joints for some geometrical parameters". *Jordan Journal of Mechanical and Industrial Engineering*, Vol 3, No 4, 2009, 236-245.
- [28] M.A. Gharaibeh, "An Accuracy and Efficiency Study on the Use of Symmetrical Numerical Models of Electronic Packages under Various Loading Conditions". *Jordan Journal of Mechanical and Industrial Engineering*, Vol 16, No. 4, 2022.
- [29] A. Arumugam, A. Pramanik, "Review of Experimental and Finite Element Analyses of Spot Weld Failures in Automotive Metal Joints". *Jordan Journal of Mechanical and Industrial Engineering*, Vol 14, No. 3, 2020.
- [30] K.V. Smith, "Application of the dissipated energy criterion to predict fatigue crack growth of Type 304 stainless steel following a tensile overload". *Engineering fracture mechanics*, Vol. 78, No.18, 2011, 3183-3195.
- [31] F. A. Al-Shamma, "The Effect of Fatigue on Crack Propagation in Flat Plates under Buckling Bending and Shear". *Jordan Journal of Mechanical and Industrial Engineering*, Vol 3, No.3, 2009.
- [32] S. Kalnaus, F. Fan, Y. Jiang, A.K. Vasudevan, "An experimental investigation of fatigue crack growth of stainless steel 304L," *International Journal of Fatigue*, Vol. 31, No. 5, 2009, 840-849.
- [33] J. Colin, A. Fatemi, S. Taheri, "Cyclic hardening and fatigue behavior of stainless steel 304L". *Journal of Materials Science*, Vol. 46, 2011, 145-154.
- [34] H. Eskandari, "Stress intensity factors for crack located at an arbitrary position in rotating FGM disks". *Jordan Journal of Mechanical and Industrial Engineering*, Vol. 8, No. 1, 2014, 27-34.
- [35] A. R. I. Kheder, N. M. Jubeh, E. M. Tahah, "Fatigue Properties under Constant Stress/Variable Stress Amplitude and Coaxing Effect of Acicular Ductile Iron and 42 CrMo4 Steel". *Jordan Journal of Mechanical and Industrial Engineering*, Vol 5, No. 4, 2011.
- [36] S. Lee, J.W. Pegues, N. Shamsaei, "Fatigue behavior and modeling for additive manufactured 304L stainless steel: The effect of surface roughness". *International Journal of Fatigue*, Vol. 141, 2020, 105856.
- [37] V. Mazánová, V. Škorik, T. Kruml, J. Polák, "Cyclic response and early damage evolution in multiaxial cyclic loading of 316L austenitic steel". *International Journal of Fatigue*, Vol. 100, 2017, 466-476.
- [38] S. Seitzl, P. Pokorný, J. Klusák, S. Duda, G. Lesiuk, "Effect of Specimen Thickness on Fatigue Crack Growth Resistance in Paris Region in AISI 304 STEEL". In *Fatigue and Fracture of Materials and Structures: Contributions from ICMFM XX and KKMP*. Cham: Springer International Publishing, 2022, 291-297.
- [39] G. Oh, A. Umezawa, "Combined loading effect on high cycle fatigue fracture behaviors of a stainless steel welded structure of elbow and socket. *International Journal of Fatigue*, 2023, 107777.
- [40] M.S. Cagle, K.E. Bryan, M. Dantin, W.M. Furr, "Characterization and modeling of the fatigue behavior of 304L stainless steel using the MultiStage Fatigue (MSF) Model". *International Journal of Fatigue*, Vol. 151, 2021, 106319.
- [41] J.Y. Huang, J.J. Yeh, S.L. Jeng, C.Y. Chen, "High-cycle fatigue behavior of type 316L stainless steel". *Materials transactions*, Vol. 47, No. 2, 2006, 409-417.
- [42] K. Solberg, S. Guan, S.M.J. Razavi, T. Welo, "Fatigue of additively manufactured 316L stainless steel: the influence of porosity and surface roughness". *Fatigue and Fracture of Engineering Materials and Structures*, Vol. 42, 2019, 2043-52.
- [43] L. Taleb, A. Hauet, "Multiscale experimental investigations about the cyclic behavior of the 304L SS". *International Journal of Fatigue*, Vol. 25, No. 7, 2009, 1359-1385.
- [44] O.M. Alyousif, R. Nishimura, "The stress corrosion cracking behavior of austenitic stainless steels in boiling magnesium chloride solutions". *Corrosion Science*, Vol. 49, 2007, 3040-3051.
- [45] X. Ling, G. Ma, "Effect of ultrasonic impact treatment on the stress corrosion cracking of 304 stainless steel welded joints". *Journal of Pressure Vessel Technology*. 2009, 131.
- [46] H. Zhang, C. Li, Y. Shi, G. Yao, "Fatigue and tensile deformation behaviors of laser powder bed fused 304L austenitic stainless steel". *Materials Science and Engineering: A*, Vol. 849, 2022, 143503.
- [47] G. Meneghetti, M. Ricotta, "The use of the specific heat loss to analyze the low-and high-cycle fatigue behaviour of plain and notched specimens made of a stainless steel". *Engineering Fracture Mechanics*, Vol. 81, 2012, 2-16.
- [48] M. Subasic, B. Alfredsson, C.F.O. Dahlberg, M. Öberg, P. Efsing, "Mechanical Characterization of Fatigue and Cyclic Plasticity of 304L Stainless Steel at Elevated Temperature". *Experimental Mechanics*, 2023, 1-17.
- [49] F. Zhou, Y. Chen, Q. Wu, "Dependence of the cyclic response of structural steel on loading history under large inelastic strains". *Journal of Constructional Steel Research*, Vol. 104, 2015, 64-73.
- [50] B. Hwang, T. Kim, Y. Kim, J. Kim, "A comparative study on hysteretic characteristics of austenitic stainless steel and carbon steel slit dampers under cyclic loading". *Journal of Building Engineering*, Vol. 45, 2022, 103553.